http://dx.doi.org/10.6113/TKPE.2013.18.4.333

불평형 비선형 부하시 궤환선형화 기법을 이용한 3상 4선식 인버터의 제어 성능 개선

보위엔뀌투[1], 이동춘†

Advanced Control of Three-Phase Four-Wire Inverters using Feedback Linearization under Unbalanced and Nonlinear Load Conditions

Nguyen Qui Tu Vo[1], and Dong-Choon Lee†

Abstract - In this paper, a feedback linearization control is proposed to regulate the output voltages of a three-phase four-wire inverter under the unbalanced and nonlinear load conditions. First, the nonlinear model of system including the output LC filters is derived in the d-q-0 synchronous reference frame. Then, the system is linearized by the multi-input multi-output feedback linearization. The tracking controllers for d-q-0-components of three-phase line-to-neutral load voltages are designed by linear control theory. The experimental results have shown that the proposed control method gives the good performance in response to the load conditions.

Keywords: feedback linearization, nonlinear load, three-phase four-wire inverter, unbalanced load

1. Introduction

Recently, the demand of the AC power supplies for standalone applications has been rapidly increased, which could be the recreational vehicles, the military trucks, or the standalone photovoltaic power systems, and so on [1]-[3]. Thus, the load conditions are often unbalanced due to the three-phase unbalanced loads, unevenly distributed single-phase loads or the balanced three-phase loads under the fault condition. These unbalanced loads cause the occurrence of the zero-sequence components in the three phase load voltages. However, the three-phase three-wire inverters cannot deal with the zero-sequence component to regulate the output voltages to be balanced. Thus, the neutral point connected to the load is required to be accessible through which the zero-sequence current can flow.

Several methods were suggested to provide the neutral point of the source side. In one category, the output Δ/Y transformer has been used [4], where the Δ and Y windings are connected to the inverter and the load, respectively. Thus, the zero-sequence current is circulated in the Δ-windings. However, the use of the transformer makes it bulky, heavy and costly. The other approaches are to use the three-phase split-capacitor inverters and the four-leg inverters. The four-leg inverter, formed by eight switches, consists of sixteen switch combinations. The four-leg inverters with the three-dimensional space vector modulation can achieve a high DC-link voltage utilization. However, the disadvantages of the four-leg inverters are the requirement of not only the additional two switches, but also the complex three-dimensional space vector modulation [5]. The three-phase split-capacitor inverters consist of the three-phase three-leg inverter and two capacitors connected in series. They are the compact and easily-implementable topologies which can take the

Paper number: TKPE-2013-18-4-5 ISSN: 1229-2214
† Corresponding author: dclee@yu.ac.kr
Dept. of Electrical Eng., Yeungnam University
Tel: +82-53-810-2582 Fax: +82-53-810-4767
[1] R&D Team, Dawonsys Co., Ltd.
Manuscript received Jan. 17, 2013; accepted Mar. 28, 2013
— 본 논문은 2012년 추계학술대회 우수추천논문임
— 본 논문은 2012년 추계학술대회 외부장학금 수혜논문임

advantages of the intelligent power modules (IPMs). Therefore, the three-phase split-capacitor inverter is a more preferable topology to provide the neutral point, even though the utilization of DC-link voltage is 15.4% less than that of four-leg inverters [2].

Several research results focusing on regulating the output voltages of the three-phase split-capacitor inverters in the unbalanced load conditions have been reported. The control strategy proposed in [6] uses a symmetrical sequence decomposition technique to extract the positive-, negative- and zero-sequence components from the unbalanced three-phase signals. Then, the dual current and voltage PI controllers for d-q axis variables of these components are applied to regulate the output voltages. However, the system dynamic response and the stability can be degraded due to the delay and errors introduced during the decomposition and composition process. In addition, this control strategy satisfies only the case of the unbalanced linear loads. Another control technique, proposed in [7], is a combination of the discrete-time sliding mode control and the robust servomechanism control in the stationary reference frame. This scheme achieved a relatively good control performance in the case of unbalanced linear and nonlinear loads. However, it is extremely difficult to locate a satisfactory sliding mode surface [8]. Besides, the selection of the state feedback gain to stabilize the system augmented by the servo compensator must be carefully considered under the load variations and parameters uncertainties [4].

A linearization technique using an input-output feedback has been applied to the DC-link voltage control of the PWM converters [9]-[10] and the line-to-line output voltage control of three-phase three-wire inverter [11] for the high dynamic responses and asymptotic tracking.

This paper proposes a novel control scheme of three-phase split-capacitor inverters using feedback linearization in the case of unbalanced linear/nonlinear loads. By applying the feedback linearization (FL) control, a decoupling control law is derived. Besides, the command tracking and dynamic stiffness performance for the FL control has been analyzed. The experimental results show the validity of the proposed control method.

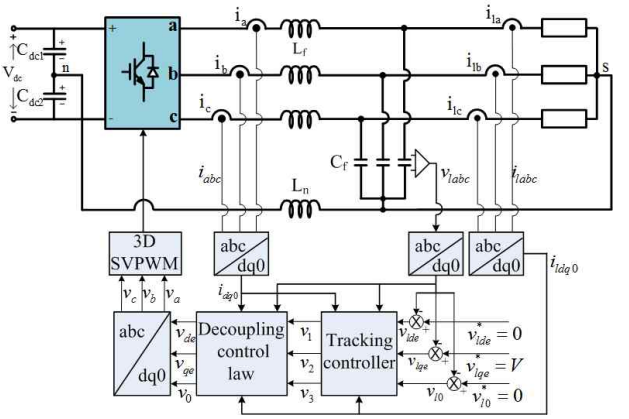

Fig. 1 A three-phase four-wire inverter and proposed control block diagram

2. System Modeling

The three-phase split-capacitor inverter, which is shown in Fig. 1, can be represented in synchronous d-q-0 reference frame. The zero-sequence component is taken into account due to the

$$\dot{i}_{dq} = \frac{1}{L_f} v_{dq} - \frac{1}{L_f} v_{ldq} - j\omega i_{dq} \tag{1}$$

$$\dot{i}_0 = \frac{1}{(L_f + 3L_n)} v_0 - \frac{1}{(L_f + 3L_n)} v_{l0} \tag{2}$$

$$\dot{v}_{ldq} = \frac{1}{C_f} i_{dq} - \frac{1}{C_f} i_{ldq} - j\omega v_{ldq} \tag{3}$$

$$\dot{v}_{l0} = \frac{1}{C_f} i_0 - \frac{1}{C_f} i_{l0} \tag{4}$$

unbalanced load condition, where L_f, L_n, and C_f are the filter inductance, the neutral filter inductance, and the filter capacitance, respectively. v_d, v_q and v_0 are the d-q-0-axis output voltages of the inverter. v_{ld}, v_{lq} and v_{l0} are the d-q-0-axis phase load voltages. i_d, i_q and i_0 are the d-q-0-axis output currents of the inverter. i_{ld}, i_{lq} and i_{l0} are the d-q-0-axis load currents. ω is the source angular frequency.

3. Feedback Linearization Control

3.1 Feedback linearization control technique

The objective of the MIMO feedback linearization approach is to eliminate the nonlinearity in the modeled system [10]. The MIMO system is expressed as:

$$\dot{x} = f(x) + g \cdot u \tag{5}$$

$$y = h(x) \tag{6}$$

where x is the state vector, u is the control input, y

is the output, f and g are the smooth vector fields, h is the smooth scalar function.

The dynamic model of three-phase four-wire inverter from (1) to (4) is expressed in (5) and (6), then

$$x=[i_d\ i_q\ i_0\ v_{ld}\ v_{lq}\ v_{l0}]^T;$$
$$u=[v_d\ v_q\ v_0]^T;$$
$$y=[v_{ld}\ v_{lq}\ v_{l0}]^T;$$
$$g=\begin{bmatrix}\frac{1}{L_fC_f} & 0 & 0\\ 0 & \frac{1}{L_fC_f} & 0\\ 0 & 0 & \frac{1}{L_fC_f}\end{bmatrix}$$
$$f(x)=\begin{bmatrix}\omega i_q-\frac{1}{L_f}v_{ld}\\ -\omega i_d-\frac{1}{L_f}v_{lq}\\ -\frac{1}{L_f+3L_0}v_{l0}\\ \frac{1}{C_f}i_d-\frac{1}{C_f}i_{ld}+\omega v_{lq}\\ \frac{1}{C_f}i_q-\frac{1}{C_f}i_{lq}-\omega v_{ld}\\ \frac{1}{C_f}i_0-\frac{1}{C_f}i_{l0}\end{bmatrix}$$

To generate an explicit relationship between the outputs $y_{i=1,2,3}$ and the inputs $u_{i=1,2,3}$ each output is differentiated until a control input appears.

$$\begin{bmatrix}\ddot{y}_1\\ \ddot{y}_2\\ \ddot{y}_3\end{bmatrix}=A(x)+E(x)\begin{bmatrix}u_1\\ u_2\\ u_3\end{bmatrix} \tag{7}$$

Then, the decoupling control law is given as

$$\begin{bmatrix}v_d^*\\ v_q^*\\ v_0^*\end{bmatrix}=\begin{bmatrix}u_1\\ u_2\\ u_3\end{bmatrix}=E^{-1}(x)\left[-A(x)+\begin{bmatrix}v_1\\ v_2\\ v_3\end{bmatrix}\right] \tag{8}$$

where

$$A(x)=\begin{bmatrix}\frac{2}{C_f}\omega i_q-\left(\frac{1}{L_fC_f}+\omega^2\right)v_{ld}-\frac{1}{C_f}\dot{i}_{ld}-\frac{1}{C_f}\omega i_{lq}\\ -\frac{2}{C_f}\omega i_d-\left(\frac{1}{L_fC_f}+\omega^2\right)v_{lq}-\frac{1}{C_f}\dot{i}_{lq}-\frac{1}{C_f}\omega i_{ld}\\ -\frac{1}{(L_f+3L_n)C_f}v_{l0}-\frac{1}{C_f}\dot{i}_{l0}\end{bmatrix}$$
$$E^{-1}(x)=\begin{bmatrix}L_fC_f & 0 & 0\\ 0 & L_fC_f & 0\\ 0 & 0 & (L_f+L_n)C_f\end{bmatrix}$$

To eliminate this tracking error in the presence of parameters variations, integral controls are added to the tracking controller. Thus, the new control inputs are given by

$$\begin{bmatrix}v_1\\ v_2\\ v_3\end{bmatrix}=\begin{bmatrix}\ddot{y}_{1ref}-k_{11}\dot{e}_1-k_{12}\dot{e}_1-k_{13}\int e_1\\ \ddot{y}_{2ref}-k_{21}\dot{e}_1-k_{22}\dot{e}_1-k_{23}\int e_2\\ \ddot{y}_{3ref}-k_{31}\dot{e}_1-k_{32}\dot{e}_1-k_{33}\int e_3\end{bmatrix} \tag{9}$$

where $e_1=y_1-y_{1ref}; e_2=y_2-y_{2ref}; e_3=y_3-y_{3ref}$.

The voltage references obtained from (8) and (9), are expressed as

$$\begin{bmatrix}u_1\\ u_2\\ u_3\end{bmatrix}=\begin{bmatrix}L_fC_fv_1-2L_f\omega i_q+\tau v_{ld}+L_f\dot{i}_{ld}+L_f\omega i_{lq}\\ L_fC_fv_2-2L_f\omega i_d+\tau v_{lq}+L_f\dot{i}_{lq}-L_f\omega i_{ld}\\ (L_f+3L_n)C_fv_3-v_{l0}+(L_f+3L_n)\dot{i}_{l0}\end{bmatrix} \tag{10}$$

where $\tau=1+L_fC_f\omega^2$.

Fig. 2 shows a process of the FL control. Fig. 2(a) illustrates the input-output relation. The nonlinearity is then eliminated by the decoupling control law as shown in Fig. 2(b). The resultant linearized system is regulated by the tracking controller in Fig. 2(c).

Each output in (7) is differentiated twice until the input appears. Thus, the total relative degree of the system is six which equals to the order of the system. There is no internal dynamics associated with the MIMO linearization. It means that the tracking controller can guarantee the stability of the overall system.

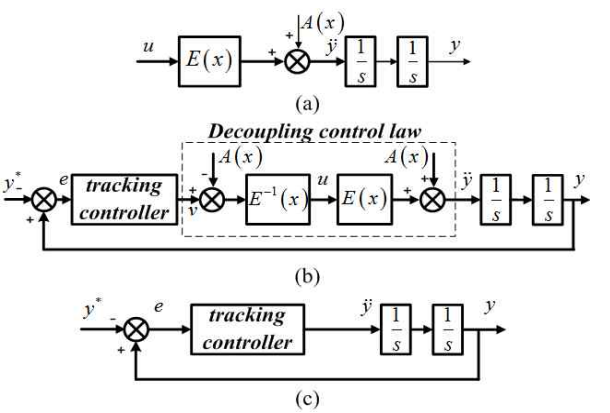

Fig. 2 A process of FL control (a) Input-output relationship (b) Decoupling control law (c) The system decoupled

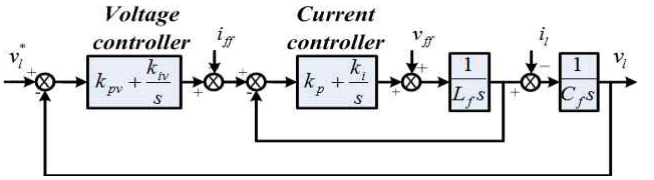

Fig. 3 Block diagram of the PI control

The closed-loop transfer function of the d-axis load voltage after decoupling is obtained as

$$\frac{v_{ld}}{v_{ld}^*} = \frac{k_{11}s^2 + k_{12}s + k_{13}}{s^3 + k_{11}s^2 + k_{12}s + k_{13}} \tag{11}$$

The variables, $k_{1j=1,2,3}$, are selected so that the polynomial, $s^3 + k_{11}s^2 + k_{12}s + k_{13}$, has all of its roots, s_1, s_2, s_3, strictly in the left-half complex plane, which leads to the exponentially stable dynamics.

The PI control technique is considered as a conventional method as shown in Fig. 3. The closed-loop transfer function is derived as

$$\frac{v_l}{v_l^*} = \frac{\sigma s^2 + k_{iv}k_p s + k_{iv}k_i}{L_f C_f s^4 + k_p C_f s^3 + \rho s^2 + k_{iv}k_p s + k_{iv}k_i} \tag{12}$$

where $\rho = k_i C_f + k_{pv}(k_p + k_i)$ and $\sigma = k_{pv}(k_p + k_i)$.

There are two basic properties which have been applied in this work to evaluate the control performance of the controllers: 1) the command tracking and 2) the dynamic stiffness. The following sections will investigate how they affect the control performance of the system.

3.2 Command tracking performance

The command tracking performance shows how the outputs track to the reference inputs. In this system the outputs are the three-phase load voltages and the inputs are the three-phase load voltage references. To get the tracking accuracy of the system to the commands, the Bode plot of the closed-loop transfer function of two controllers is analyzed in Fig. 4. As can be seen, the two controllers have a unity gain

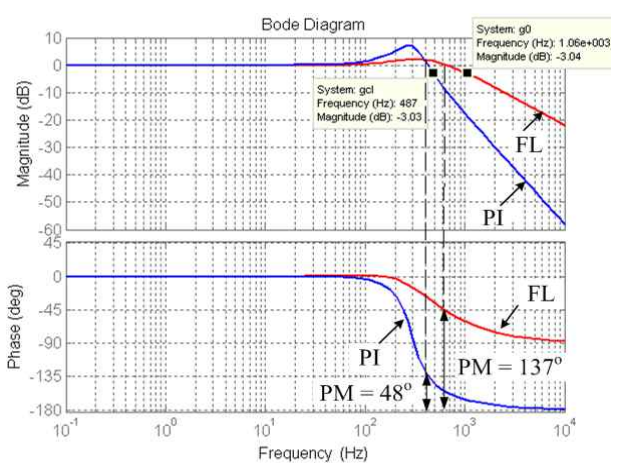

Fig. 4 Bode plot of the FL and PI controls

and zero phase delay at the low frequency range, which gives the good tracking accuracy of controllers. The positive values of the phase and gain margins ensure the stability property of the controllers. The FL control has a lower resonant peak and a wider bandwidth which result in the lower overshoot and the faster settling time at the stepwise load change. Thus, the command tracking performance [14] of the FL control is better than that of the PI control. The experimental results illustrated in the Fig.10 to Fig.15 also show the better command tracking performance of the FL control.

3.3 Dynamic stiffness property

The dynamic stiffness of a system is defined as the ratio of the process disturbance to the process output [14]-[16]. It represents the effect of the process disturbance on the outputs. In this system, the action of providing inverter output voltages to response to the change of load for balancing the load voltages is equivalent to providing dynamic stiffness. The system, which is shown in Fig. 5(a), consists of the three-phase split-capacitor inverter with the LC output filter which connects to the load. The load current varieswith the type of loads which are the unbalanced linear and nonlinear loads. Hence, the load current is considered as a process disturbance. The block diagram of the three-phase split-capacitor inverter with the LC output filter is shown in Fig. 5(b). The dynamic stiffness of the system without any controller is expressed as

$$\frac{I_l(s)}{V_l(s)} = \frac{L_f C_f s + 1}{L_f s} \tag{13}$$

As mentioned earlier, Fig. 3 shows the system applying the PI current and voltage controllers. The load current is also considered as a disturbance. Hence, the dynamic stiffness can be derived as

$$\frac{I_l(s)}{V_l(s)} = \frac{L_f C_f s^4 + k_p C_f s^3 + \rho s^2 + k_{iv}k_p s + k_{iv}k_i}{L_f s^3 + k_p s^2 + k_i s} \tag{14}$$

In the process of the FL control, the change of load current is calculated by the matrix $A(x)$ and then is cancelled by the decoupling control law as shown in Fig. 2(b). In the presence of the load change or the parameter variations, there may exist an error $D(s)$

of the decoupling control law which is considered as a process disturbance. Therefore, the dynamic stiffness of the FL control is derived as follows:

$$\frac{D(s)}{V_l(s)} = \frac{Ls^3 + k_{11}s^2 + k_{12}s + k_{13_i}}{s} \tag{15}$$

The dynamic stiffness property of the FL and PI controls is shown in Fig. 6. The dynamic stiffness of the FL control is significantly improved in comparison with PI control. Thus, the FL control gives better performance at the disturbance rejection.

4. 3-D Space Vector Modulation

The application of 3-D SVM for a three-phase split-capacitor PWM inverter was presented in [17]. The space vectors, switching states and inverter output voltages were described in detail in [13]. Due to the presence of the zero-sequence component, the eight basic space vectors are distributed in the α-β-0 space which is shown in Fig. 7(a). Hence, the inverter output voltage reference vector is expressed by 3-D vectors as follows:

$$\overrightarrow{V_R} = i \cdot v_{R\alpha} + j \cdot v_{R\beta} + k \cdot v_{R0} \tag{16}$$

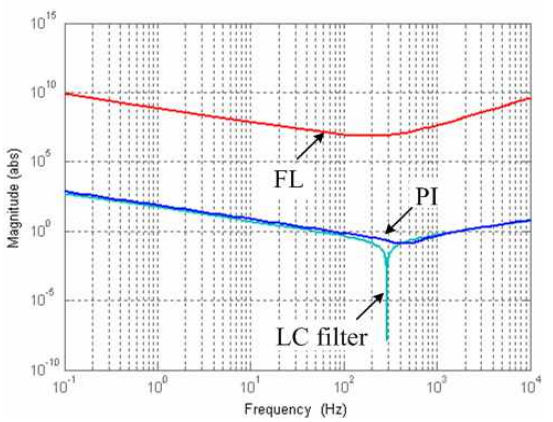

Fig. 5 Three-phase split-capacitor inverter with LC output filter (a) The equivalent circuit (b) the block diagram

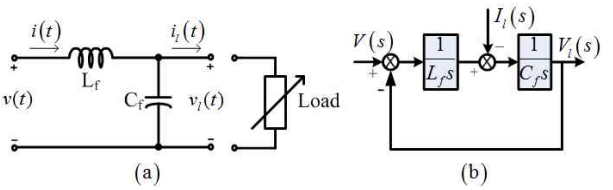

Fig. 6 Dynamic stiffness property of the FL and PI controls

The reference vector $\overrightarrow{V_R}$ is projected into the α-β plane as shown in Fig. 7(b). Then, it can be synthesized by its adjacent vectors $\overrightarrow{V_1}$, $\overrightarrow{V_2}$, $\overrightarrow{V_7}$ and $\overrightarrow{V_8}$ in the α-β plane

$$\begin{aligned} V_1T_1 + V_2T_2 + V_7T_7 + V_8T_8 &= V_RT_s \\ T_1 + T_2 + T_7 + T_8 &= T_s \end{aligned} \tag{17}$$

where T_s is the sampling frequency. The effective times of each space vector for the sector I are calculated by (18). For the other sectors, the equations are also obtained by the similar manner [13]. Fig. 8 illustrates the switching sequence for the reference voltage in the sector I.

$$\begin{aligned} T_1 &= \frac{\sqrt{3}\,T_s}{V_{dc}}\left(\frac{\sqrt{3}}{2}v_{R\alpha} - \frac{1}{2}v_{R\beta}\right) \\ T_2 &= \frac{\sqrt{3}\,T_s}{V_{dc}}v_{R\beta} \\ T_7 - T_8 &= \frac{2v_{R0}}{V_{dc}}T_s - \frac{1}{3}(T_2 - T_1) \\ T_7 + T_8 &= T_s - T_1 - T_2 \end{aligned} \tag{18}$$

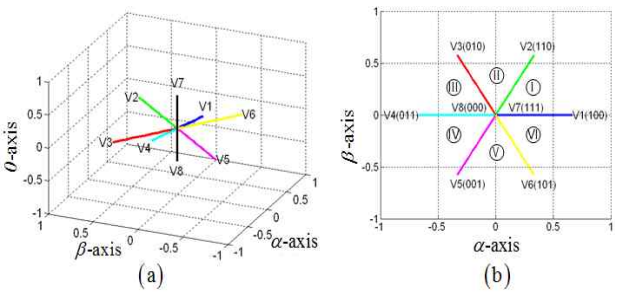

Fig. 7 Eight space vectors of three-phase split-capacitor inverter (a) in the α-β-0 space (b) projected in the α-β plane

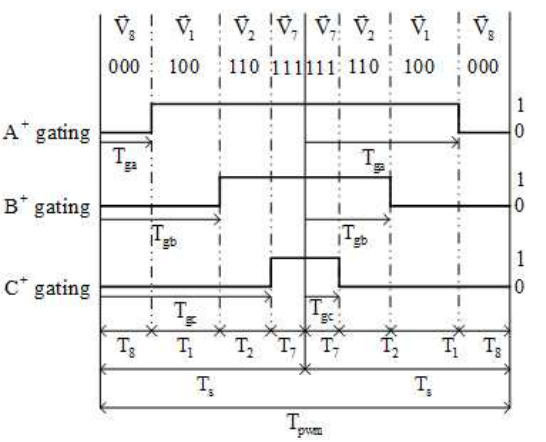

Fig. 8 Switching sequence for the reference vector in the sector

It should be noted that the inequality of T_7 and T_8 is used for synthesizing the zero-sequence voltages to balance the three-phase line-to-neutral load voltages. Thus, the inverter control can be performed in the α-β-0 three dimensional coordinate.

5. Experimental Results

The validity of the proposed control algorithm has been verified by experimental tests for the unbalanced linear and nonlinear loads. The three-phase four-wire split capacitor inverter was setup by the intelligent power module (PM75RLA060) and two DC-link capacitors. A three-phase diode rectifier is used to supply *300*[V] DC-link voltage at the input of inverter from a three-phase AC source. The switching frequency of the inverter is selected as *10*[kHz] for harmonic reduction [18],[19]. The filter inductor, L_f , is *3*[mH] and the filter capacitor, C_f ,is *100*[μF] which correspond to a cut-off frequency at *450*[Hz]. The layout of the experimental set-up is shown in the Fig. 9. The parameters of the loads and controllers are listed in the Table 2 and Table 3, respectively. It should be noted that the PI control method needs to adjust the controller gains for other types of loads. On the contrary, the FL control can achieve the good performance without adjusting the gains in the both cases of unbalanced linear and nonlinear loads.

Table 2 Parameters of loads

Type of load	Parameters
Unbalanced resistor load	$R_a = R_b = 20$ [Ω] $R_c = 1$ [kΩ]
Unbalanced nonlinear load	$L_s = 1$ [mH], C = 4.7 [mF], $R_{dca} = 50$ [Ω], $R_{deb}=R_{dcc}=1$ [kΩ]

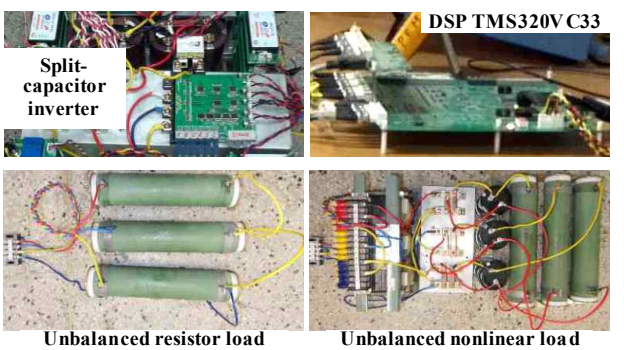

Fig. 9 The layout of the experimental set-up

Table 3 Parameters of controllers

Controller type		Controller gains	
		Unbalanced linear load	Unbalanced nonlinear load
PI control	Current controller	$k_p = 11.4$ $k_i = 38$	$k_p = 7.5$ $k_i = 25$
	Voltage controller	$k_{pv} = 0.31$ $k_{iv} = 484$	$k_{pv} = 0.2$ $k_{iv} = 196$
FL control		$k_1 = 5.1 \times 10^3$ $k_2 = 8.67 \times 10^6$ $k_3 = 4.913 \times 10^9$	

Fig. 10 to Fig. 13 show the experimental results of the FL and PI control at unbalanced linear and nonlinear loads. Each figure illustrates the three-phase line-to-neutral output voltages, three-phase load currents, zero-sequence current and DC link capacitors voltages. As can be seen, the three-phase line-to-neutral output voltages are maintained to be balanced. Their total harmonic distortion (THD) values are recorded in the Table 4. It should be noted that the command tracking performance, with respect to the THD of the two controllers is not so different, in the case of unbalanced linear loads. However, the THD of the phase-A load voltage in the case of PI control is significantly increased by 6.0%, in the case of unbalanced nonlinear load while that of FL control is kept at 2.3%. The FL control with higher dynamic stiffness achieves better control performance than the PI control in the case of the unbalanced nonlinear load.

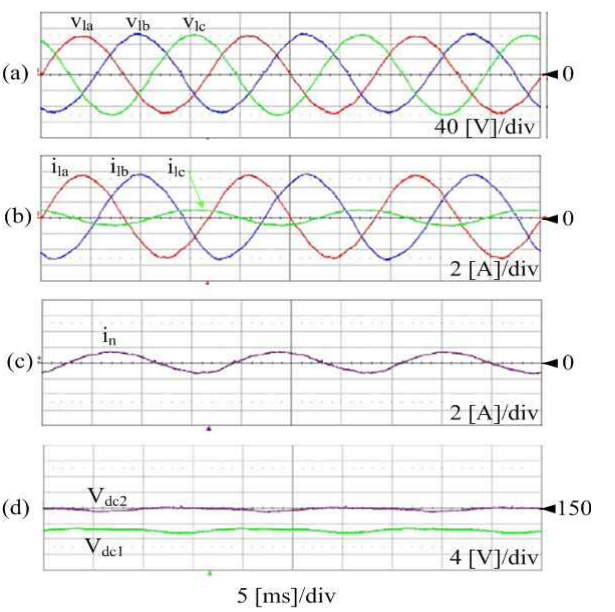

Fig. 10 Performance of the FL control under the unbalanced linear load (a) Three-phase load voltages (b) Three-phase load currents (c) Neutral-line current (d) DC-link capacitor voltages

Fig. 14 and Fig. 15 show the response of controllers to the step change of resistor load. A set of the analog timer (AT8SDN) and solid state relay (SDA3-260R) is setup to provide the sequence of abrupt changes from the full load to no load and vice versa, after 50[ms]. In Fig. 13(a) and (b), the waveforms

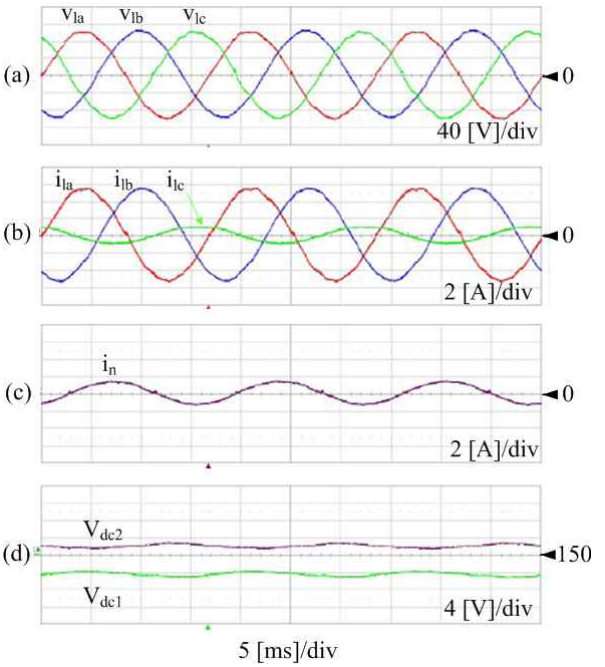

Fig. 11 Performance of the PI control under the unbalanced linear load (a) Three-phase load voltages (b) Three-phase load currents (c) Neutral-line current (d) DC-link capacitor voltages

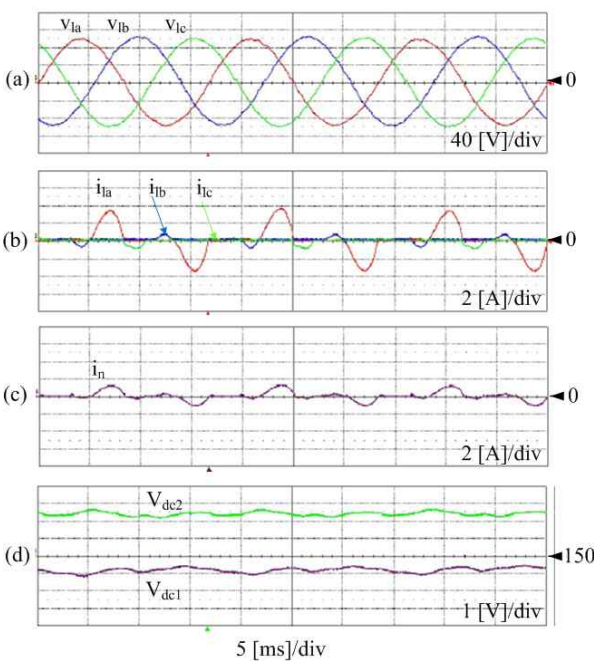

Fig. 12 Performance of the FL control under unbalanced nonlinear load (a) Three-phase load voltages (b) Three-phase load currents (c) Neutral-line current (d) DC-link capacitor voltages

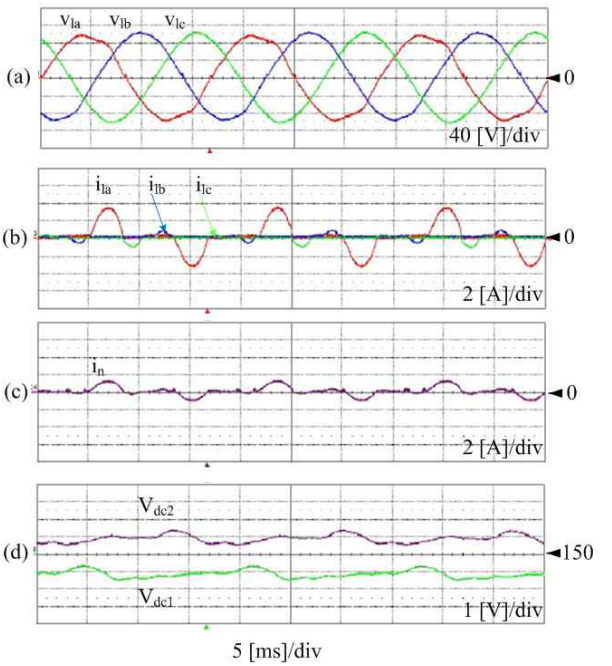

Fig. 13 Performance of the PI control under unbalanced nonlinear load (a) Three-phase load voltages (b) Three-phase load currents (c) Neutral-line current (d) DC-link capacitor voltages

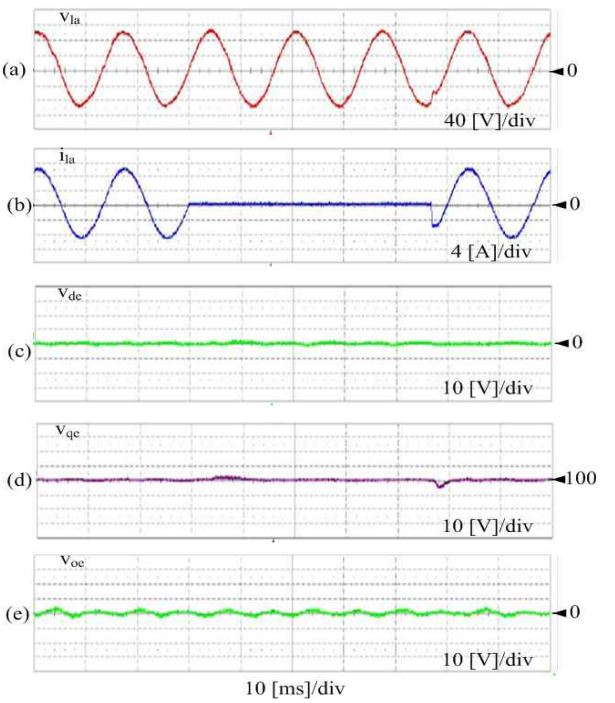

Fig. 14 FL control at load step changes (a) Phase-A load voltage (b) Phase-A load current (c) d-axis load voltage (d) q-axis load voltage (e) 0-axis load voltage

Table 4 THD of load voltages

Load type	Controller type	THDa [%]	THDb [%]	THDc [%]
Unbalanced linear load	PI control	2.8	2.0	3.4
	FL control	2.5	2.8	2.2
Unbalanced nonlinear load	PI control	6.0	2.8	2.2
	FL control	2.3	2.0	1.8

of phase-A load voltage and current are shown. The responses of d-q-0 axis voltages for the step change of load are also shown in Fig. 13 (c)-(e). Compared with the results of the PI control in Fig. 14(c)-(e), the FL control obviously show the faster response performance to the stepwise load change with respect to the lower overshoots and shorter settling time.

6. Conclusions

This paper has proposed a novel output voltage control of the three-phase split-capacitor inverter using a multivariable feedback linearization. The FL control can regulate the load voltages to be balanced in the case of the unbalanced linear and nonlinear loads. In addition, the comprehensive analysis in the frequency domain for the FL and PI controls has been presented. The feasibility of the FL control for the three-phase split-capacitor inverter has been verified by the experimental results, which show the better performance than the conventional PI control method.

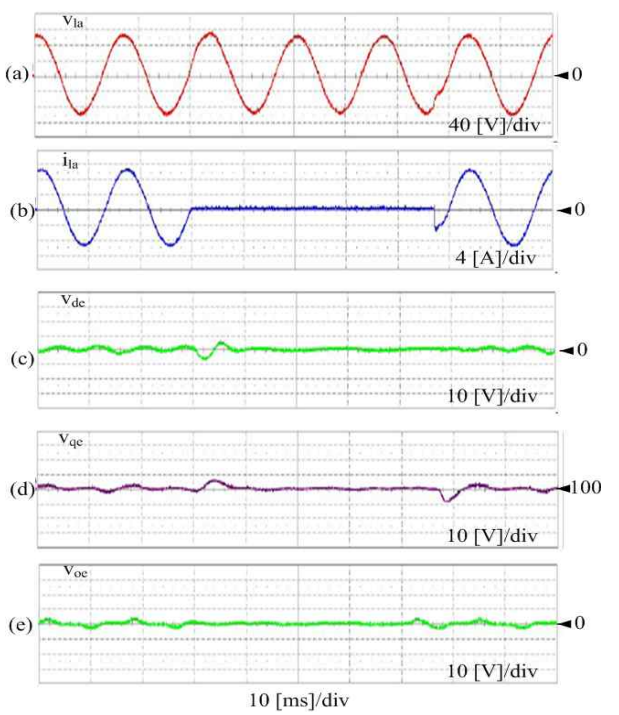

Fig. 15 PI control at load step changes (a) Phase-A load voltage (b) Phase-A load currents (c) d-axis load voltage (d) q-axis load voltage (e) 0-axis load voltage

Acknowledgement

This research was supported by Basic Science Research Program through the National Research Foundation of Korea(NRF) funded by the Ministry of Education, Science and Technology (NRF-2012 R1A1A4A01015362).

References

[1] Y.-C. Jeung and D.-C. Lee, "AC Power Supply System using Vehicle Engine-Generator Set with Battery," *in Proc. of IPEMC (ECCE-Asia)*, pp. 1724-1728, Jun. 2012.

[2] R. Zhang, D. Boroyevich, V. H. Prasad, H. Mao, F. C. Lee, andS. Dubovsky, "A Three-Phase Inverter with A Neutral Leg with Space Vector Modulation," *in Proc. of IEEE APEC*, Vol. 2, pp. 857-863, Feb. 1997.

[3] S. El-Barbari and W. Hofmann, "Digital Control of a Four Leg Inverter for Standalone Photovoltaic Systems with Unbalanced Load," *in Proc. of IEEE IECON*, pp. 729-734, 2000.

[4] M. N. Marwali, M. Dai, and A. Keyhani, "Robust Stability Analysis of Voltage and Current Control for Distributed Generation Systems," *IEEE Trans. on Energy Convers.*, Vol. 21, No. 2, pp. 516-526, Jan. 2006.

[5] R. Zhang, H. Prasad, D. Boroyevich, and F. C. Lee, "Three-Dimensional Space Vector Modulation for Four-Leg Voltage-Source Converters," *IEEE Trans. on Power Electron.*, Vol. 17, No. 3, pp. 314-326, May 2002.

[6] A. Mohd, E. Ortjohann, N. Hamsic, W.Sinsukthavorn, M. Lingemann, A. Schmelter, and D. Morton, "Control Strategy and Space Vector Modulation for Three-Leg Four-Wire Voltage Source Inverters under Unbalanced Load Conditions," *IET Power Electronics*, Vol. 3, No. 3, pp. 323-333, 2010.

[7 M. Dai, M. N. Marwali, J.-W. Jung and A. Keyhani, "A Three-Phase Four-Wire Inverter Control Technique for a Single Distributed Generation Unit in Island Mode," *IEEE Trans. on Power Electron.*, Vol. 23, No. 1, pp. 322-331, Jan. 2008.

[8] S. L. Jung and Y. Y. Tzou, "Discrete Sliding-Mode Control of a PWM Inverter for Sinusoidal Output Waveform Synthesis with Optimal Sliding Curve," *IEEE Trans. on Power Electron.*, Vol. 11, No. 4, pp. 567-577, Jul. 1996.

[9] L. Yacoubi, K. Al-Haddad, L.-A. Dessaint, and F. Fnaiech, "A DSP-Based Implementation of a New Nonlinear Control for a Three-Phase Neutral Point Clamped Boost Rectifier Prototype," *IEEE Trans. Ind. Electron.*, Vol. 52, No. 1, pp. 197 - 205, Feb. 2005.
[10] D.-C. Lee, G.-M. Lee, and K.-D. Lee, "DC-Bus Voltage Control of Three-Phase AC/DC PWM Converters Using Feedback Linearization," *IEEE Trans. Ind. Appl.*, Vol. 36, No. 3, pp. 826 - 833, May/Jun. 2000.
[11] D.-E. Kim and D.-C. Lee, "Feedback Linearization Control of Three-Phase UPS Inverter Systems," *IEEE Trans. Ind. Electron.*, Vol. 57, No. 3, pp. 963 - 968, Mar. 2010.
[12] J.-J. E. Slotine and W. Li, Applied Nonlinear Control. Englewood Cliffs, NJ: Prentice-Hall, pp. 207 - 271, 1991.
[13] N. Q. T. Vo and D.-C. Lee, "Nonlinear Control of Three-phase Split-Capacitor Inverters under Unbalanced and Nonlinear Load Conditions," *KIPE 2012 Power Electronics Autumn Conf.*, pp. 52-53, Nov. 2012.
[14] R. D. Lorenz, T. A. Lipo, and D.W. Novotny, "Motion Control with Induction Motors," *in Proc. of IEEE*, Vol. 82, pp. 1215-1240, 1994.
[15] R. D. Lorenz and P. B. Schmidt, "Synchronized Motion Control for Process Automation," *in Proc. of IEEE IAS*, Vol. 2, pp. 1693-1698, 1989.
[16] D.-K. Ku, J.-K. Ji, G.-S. Cha, and J.-H. Moon, "Design of Robust Voltage Controller for Single-Phase UPS Inverter," *The Transaction of the Korean Institute of Power Electronics.*, Vol. 16, No. 4, pp. 317 - 325, Aug. 2011.
[17] C. Zhan, A. Arulampalam, V. K. Ramachandaramurthy, C. Fitzer, M. Barnes, and N. Jenkins, "Novel Voltage Space Vector PWM Algorithm of 3-Phase 4-Wire Power Conditioner," *in Proc. of IEEE PES Winter Meeting*, pp. 1045-1050, 2001.
[18] T.-K. Vu, S. Lee, and H.-J. Cha, "A New On-Line Dead-Time Compensator for Single-Phase PV Inverter," *The Transaction of the Korean Institute of Power Electronics.*, Vol. 17, No. 5, pp. 409 - 415, Oct. 2012.
[19] H.-M. Oh, S.-W. Choi, T.-H. Kim, G.-P. Lee, and T.-W. Lee, "Anti-islanding Method by Harmonic Injection for Utility Interactive Inverter with Critical Load," *The Transaction of the Korean Institute of Power Electronics.*, Vol. 17, No. 4, pp. 315 - 321, Aug. 2012.

Nguyen Qui Tu Vo was born in Quang Ngai, Viet Nam in 1984. He received his B.S. in Engineering from the Ho Chi Minh City University of Technology, in 2007 and his M.S. in the Department of Electrical Engineering, Yeungnam University, Korea in 2013. He is currently with the R&D Team in the Dawonsys company, Korea. His research interests include power converters control and power circuit design.

Dong-Choon Lee received his B.S., M.S., and Ph.D. in Electrical Engineering from Seoul National University, Seoul, Korea, in 1985, 1987, and 1993, respectively. He was a Research Engineer with Daewoo Heavy Industry from 1987 to 1988. Since 1994, he has been a Faculty Member in the Department of Electrical Engineering,Yeungnam University, Gyeongbuk, Korea. As a Visiting Scholar, he joined the Power Quality Laboratory, Texas A&M University, College Station in 1998, and the Electrical Drive Center, University of Nottingham, U.K. in 2001, and the Wisconsin Electric Machines and Power Electronic Consortium, University of Wisconsin, Madison in 2004, and the FREEDM Systems Center, North Carolina State University, Raleigh from September, 2011 to August, 2012. Currently, he is a Publication Editor of Journal of Power Electronics. His research interests include ac machine drives, control of power converters, wind power generation, and power quality.